Ferrite and Bainite in Alloy Steels

R. W. K. HONEYCOMBE AND F. B. PICKERING

The addition of alloying elements even in small concentrations can alter the properties and structure of ferrite and bainite. The various morphologies of ferrite-carbide aggregates are surveyed including alloy pearlite, fibrous carbide eutectoids and precipitation of fine alloy carbides at γ-α interfaces. Modern ideas on the morphology and growth kinetics of ferrite and upper and lower bainite are also summarized. Using this information, an attempt is made to rationalize subcritical transformations of austenite in low alloy steels. Basic factors influencing the strength of alloy ferrites are discussed, leading to an examination of structure-mechanical property relationships in ferrite and bainite. Finally the exploitation of the ferrite and bainite reactions to produce useful alloy steels by direct transformation of austenite is explored.

THE decade before World War II was one of the most fruitful in the development of our understanding of the heat treatment of steels. This was in no small measure due to the efforts of a group of American metallurgists both in industry and universities, who laid the foundations of the metallurgy of heat treatment. Edgar Bain, whose eightieth birthday we are celebrating with this seminar, was an outstanding figure in this period, who by his classical work on isothermal transformation of steels provided the framework on which the present day technology of heat treatment is based. Bain successfully bridged the gap between academic enquiry and the application of scientific principles to the development of steels in a way which has earned the enduring respect of succeeding generations of metallurgists in many countries. With other pioneers such as Martens, Roberts-Austen, and Widmanstätten, his name will always be enshrined in the nomenclature of the subject.

The present paper discusses some aspects of ferritic and bainitic microstructures in an effort to relate these to the mechanical properties of alloy steels. We have chosen to deal with both ferrite and bainite together because of the difficulty in defining the demarcation between the two categories of structure in practice. The subject is a microcosm of physical metallurgy, in so far as it covers the whole spectrum of transformation and precipitation reactions, including both diffusion-controlled and shear transformations, nucleation of precipitates on interfaces, dislocations and grain boundaries, and the cooperative growth of both precipitate and major phase.

MORPHOLOGY AND CRYSTALLOGRAPHY OF FERRITIC AND BAINITIC REACTIONS

There is a complex series of transformation products formed in alloy austenite as a result of decomposition at subcritical temperatures, ranging from polyhedral ferrite at the higher temperatures through Widmanstätten ferrite, to upper, then lower bainite at the lowest temperatures. At most stages carbide precipitation accompanies ferrite formation because of the lower solubility of carbon in ferrite than in austenite. All the structures are aggregates of ferrite and carbides, but the carbide and ferrite compositions on the one hand, and their microstructure on the other, change both with the transformation and the composition of the steel. We shall now discuss each reaction product in turn, commencing at the higher transformation temperatures.

1) Polyhedral Ferrite

In plain carbon steels at high transformation temperatures (750° to 850°C) ferrite nucleates at the austenite grain boundaries in several massive morphologies classified by Mehl and Dubé.[1-3] These ferrite areas are largely free from carbide. Similar structures appear in a wide range of alloy steels exemplified by a simple vanadium steel, Fig. 1. Whereas in the plain carbon steels, the carbide forms either as discrete cementite particles or in pearlite nodules after substantial ferrite growth, in alloy steels containing strong carbide formers the ferrite growth is often restricted by the need of alloying elements to partition by diffusion. The result is that ferrite and carbides frequently coprecipitate even in low carbon steels. The alloying element often results in a composition which is basically hypereutectoid, in so far as

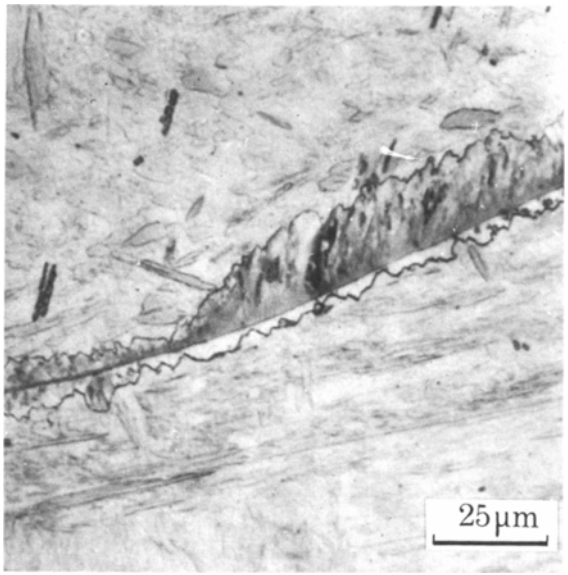

Fig. 1—An Fe-2 pct V-0.2 pct C alloy isothermally transformed for 10 sec at 650°C. Optical micrograph, magnification 600 times. (Davenport and Honeycombe).

R. W. K. HONEYCOMBE is Professor, Department of Metallurgy, University of Cambridge, Cambridge, England. F. B. PICKERING is with the British Steel Corp., Southmede, Rotherham, England.

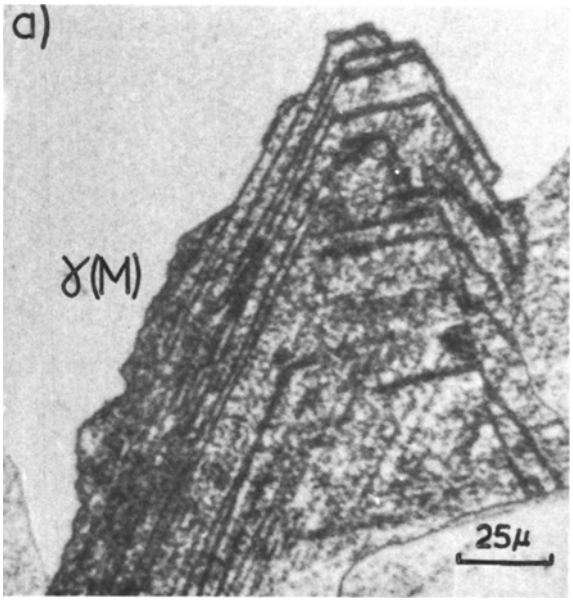

Fig. 2—An Fe-6 pct W-0.23 pct C alloy partially transformed after 2 hr at 800°C. Optical micrograph, magnification 500 times. (Davenport and Honeycombe).

alloy carbide *under equilibrium conditions* would be expected to form first at the austenite grain boundaries.

Observations on numerous alloy steels indicate that the presence of alloying elements in solid solution does not markedly alter the observed morphologies of ferrite. The kinetics of the reaction can, however, be substantially influenced. As emphasized by Smith,[4] the ferrite usually has an orientation relationship with one of the austenite grains, viz. Kurdjumov-Sachs relation,[5]

$$\{111\}_\gamma \parallel \{110\}_\alpha$$

$$\langle 110\rangle_\gamma \parallel \langle 111\rangle_\alpha$$

and a random relationship with the other. Thus characteristic variations in morphology can develop on each side of a ferrite crystal as the conditions of transformation change. For example, the γ-α boundary on the orientation-related side can develop a sawtooth morphology, which can further degenerate into a marked plate-like growth (side plates) which is effectively a form of Widmanstätten ferrite. On the other side, the γ-α boundary, being a high energy incoherent interface, provides favored sites for the nucleation of pearlite, the ferrite of which has been shown *not* to be related to the grain in which it is growing, but to the *adjacent* austenite grain.[6]

Side-plate ferrite grows rapidly in the edge-wise direction, but because the planar γ-α boundary is coherent and intrinsically not mobile, it grows slowly in the direction perpendicular to this boundary. However, this difficulty, frequently met in phase transformations, has been overcome by assuming that the ferrite grows by the propagation of ledges along the coherent interfaces.[7] The ledges need not be very large, and thus can be difficult to observe; however they are readily seen in certain systems, *e.g.* Fe-W-C[8] and Fe-Cr-C.[9] An example of coarse ledge formation in ferrite in an Fe-6 pct W-0.23 pct C alloy is shown in Fig. 2.

Growth of the disordered ferrite boundary on the other side of the ferrite allotriomorph presents little difficulty in so far as it is a high energy boundary which can grow rapidly by atomic transfer across the γ-α interface.

2) Pearlite and Related Structures

Proeutectoid ferrite and pearlite are well-defined phases in plain Fe-C alloys, and in steels containing noncarbide formers such as nickel. However, in the presence of increasingly strong carbide formers such as Cr, Mo, V, and Ti, ferrite and pearlite can be to a large degree replaced by complex aggregates of ferrite and alloy carbides. Apart from classical pearlitic structures in which the alloying element is present both in the ferrite and the cementite, there are at least three distinguishable forms of ferrite-carbide aggregates which occur in the temperature range above where upper bainite forms.

2.1) Pearlitic-Type Structures

Addition of alloying elements in solid solution in austenite, *e.g.* molybdenum, chromium, has a large influence on the nucleation and growth of pearlite nodules. For example 0.5 pct Mo decreases the growth rate of pearlite in the range 600° to 700°C by a factor of more than 100. Cahn and Hagel[10] have pointed out that the diffusion of carbon in both austenite and ferrite is not significantly altered by small concentrations of other alloying elements, so the observed effect on growth of pearlite must be due either to partitioning or to interfacial effects. Strong carbide-forming elements such as Cr, V, Mo, W will partition to the cementite, while Co, Ni, and Si partition to the ferrite. Consequently in many cases cementite will, at a critical concentration, be replaced by an alloy carbide.[11] For example, Mehl and Hagel[12] have shown that with increasing molybdenum content, $(Fe\ Mo)_{23}C_6$ replaces cementite in pearlite, while in high chromium steels $(Cr\ Fe)_{23}C_6$ replaces cementite.

These alloy carbide pearlites, which have not received much detailed structural study, are usually only encountered at the higher transformation temperatures, just below Ae_1, where reaction rates tend to be slow, *i.e.* in circumstances where partition of alloying element is most likely to take place. A good example is found in a 12 pct Cr, 0.2 pct C steel transformed for several minutes at 750°C in which alloy pearlite is formed with $Cr_{23}C_6$ laths.[9,13] Fig. 3 shows such a structure, which although coarse, is much finer in scale than cementitic pearlite formed at the same temperature.

2.2) Fibrous Carbide–Ferrite Structures

These frequently occur as nodules or fringes nucleating at austenite grain boundaries[14-16] in which the fibrous carbides are usually several μm long and between 10–50 nm (100 to 500Å) diameter, occurring in parallel arrays or tufts. A typical occurrence in a molybdenum steel has been shown in Fig. 4, where the carbide was identified as Mo_2C. There is now little doubt that this fibrous morphology is one which many different carbides can adopt, *e.g.* Mo_2C, V_4C_3, TiC, Cr_7C_3, W_2C, and that it is normally associated with

Fig. 3—An Fe-12 pct Cr-0.2 pct C alloy isothermally transformed 15 min at 750°C. Coarse laths of $M_{23}C_6$. Thin foil electron micrograph, magnification 31,000 times. (Campbell).

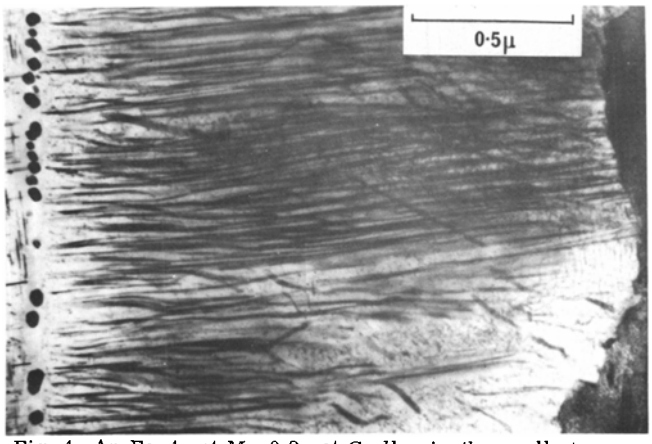

Fig. 4—An Fe-4 pct Mo-0.2 pct C alloy isothermally transformed 30 min at 700°C. Fibrous Mo_2C. Thin foil electron micrograph, magnification 42,600 times. (Berry).

ferrite in pearlite-type nodules growing from austenite grain boundaries in alloy steels. Indeed, while coarse lamellar alloy carbide pearlites can occur in some steels at high transformation temperatures, it is evident that the fibrous carbide/ferrite aggregates are very typical of the behavior of alloy carbides participating in the normal type of eutectoid decomposition, where the ferrite of the transformation product is not related to the austenite grain in which it is growing.

Detailed work on 4 pct Mo steels by Berry[16] has shown that fibrous Mo_2C-ferrite aggregates are a common transformation product in the temperature range 600° to 800°C, provided the carbon content is low (< 0.3 pct). At higher carbon levels there is insufficient molybdenum to ensure that only Mo_2C forms,

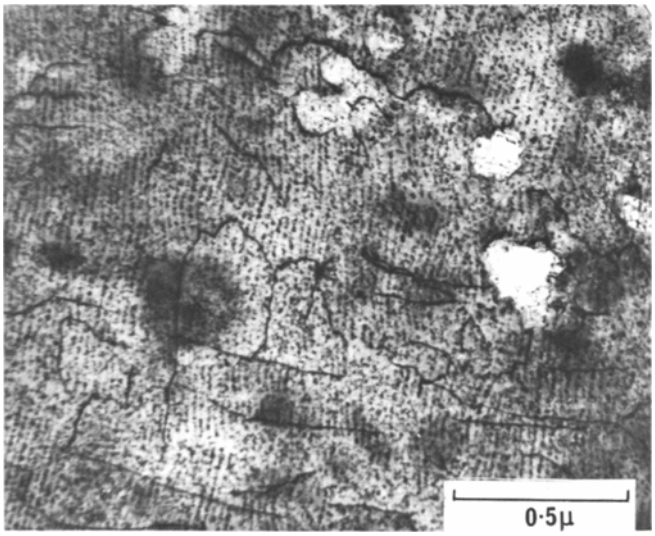

Fig. 5—An Fe-0.25 pct Ti-0.2 pct C alloy solution treated at 1320°C, transformed, then held $4\frac{1}{2}$ days at 710°C. Thin foil electron micrograph, magnification 46,000 times. (Freeman).

so the formation of the fibrous eutectoid occurs first and subsequently coarser pearlite structures are obtained. These structural studies have shown that the orientation relationships between the austenite, ferrite, and carbide are such that the carbide fibers must have nucleated in contact with austenite. Close examination of the interface reveals that both the carbide fibers and the ferrite are in direct contact with the austenite.

Similar fibrous morphologies have been observed in tungsten steels[8] and in vanadium steels,[17] usually at the higher transformation temperatures, but in the case of molybdenum steels at temperatures as low as 650°C, well below the nose in the *TTT* diagram. In the vanadium steels, the fibrous carbide did not occur at all except at transformation temperatures around 800°C, until the reaction was slowed down by the addition of manganese or nickel.

It is difficult to make a clear-cut distinction between these fiber-carbide aggregates and the pearlitic structures described earlier except in terms of the dimensions of the fibers, which tend to be an order of magnitude finer than the pearlitic carbide laths formed under comparable conditions. It appears likely that the finer fibrous form is more readily adopted by the carbides of simpler crystal structure, *e.g.* Mo_2C, V_4C_3, which are not always the equilibrium carbides at high transformation temperatures. The equilibrium carbides tend to be of the types $M_{23}C_6$ or M_6C, with more complex unit cells, and these often adopt the less precise morphology characteristic of pearlite.

2.3) Interphase Precipitation

In this structure[8,13,18,19,23] the ferrite frequently adopts one of the familiar morphologies of carbide-free ferrite, but contains closely spaced bands of fine alloy carbides (interphase precipitation). This morphology has been observed in steels containing V,[8] W,[8] Mo,[16] Ti,[20] and Cr.[9,13] Vanadium and titanium steels transformed in the range 650° to 800°C exhibit particularly fine-banded dispersions of vanadium or titanium carbides.[8,21] These dispersions have several

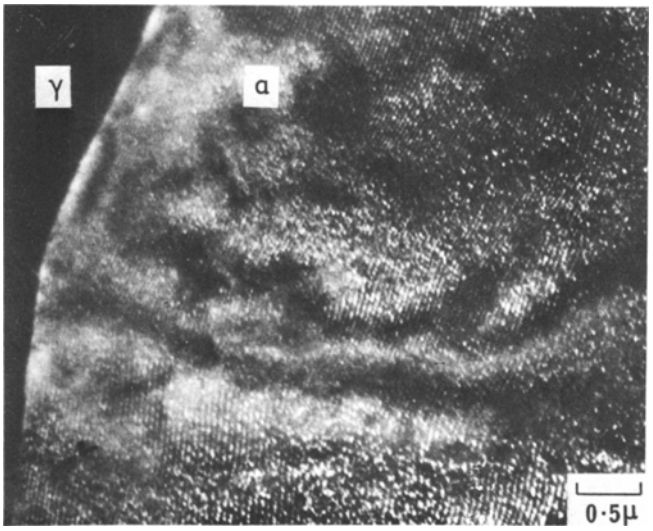

Fig. 6—An Fe-1 pct V-0.2 pct C alloy with 3 pct Ni, transformed 5 min at 690°C. The vanadium carbide particles are illuminated in dark field and the γ-α boundary is shown. D. F. electron micrograph using V_4C_3 reflection, magnification 86,000 times. (Davenport and Honeycombe).

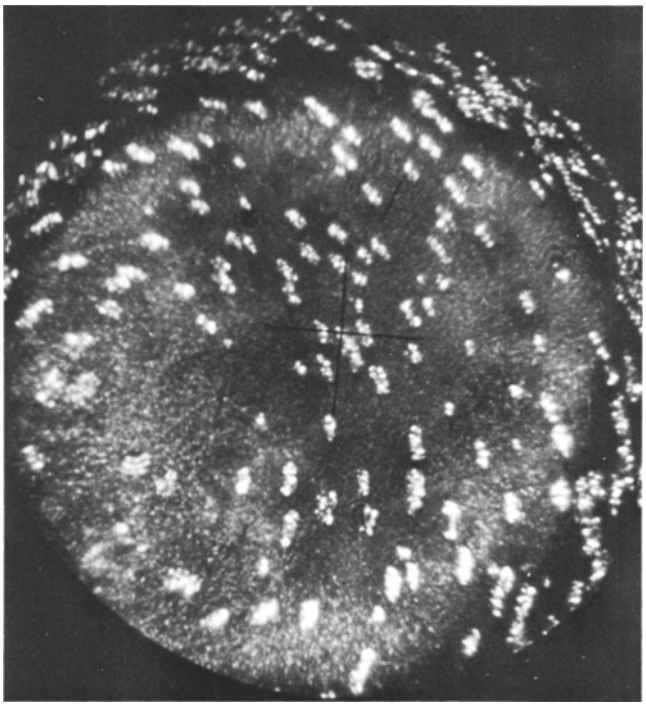

Fig. 7—An Fe-1 pct V-0.2 pct C alloy transformed $3\frac{1}{2}$ hr at 650°C to coarsen precipitate. V_4C_3 particles in ferrite: pole of habit of precipitate is $(100)_\alpha$. Field ion micrograph, magnification ~ 800,000 times. (Schwartz and Ralph).

unusual characteristics which distinguish them from normal precipitation in a supersaturated solid solution. They are:

1) The precipitate is not randomly dispersed, but is present in fine parallel bands. Fig. 5 shows such a structure in a steel containing 0.25 pct Ti and 0.1 pct C which has been transformed at 710°C, then held at this temperature $4\frac{1}{2}$ days to coarsen the precipitate. Immediately after transformation in the temperature range 650° to 700°C the spacing of the bands can be in the range 5 to 10 nm (50 to 100Å). Fig. 6 is a dark field image of a steel containing 1 pct V and 0.2 pct C

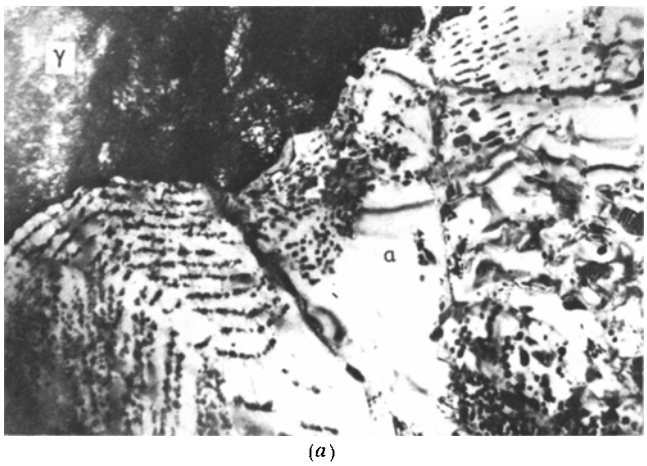

(*a*)

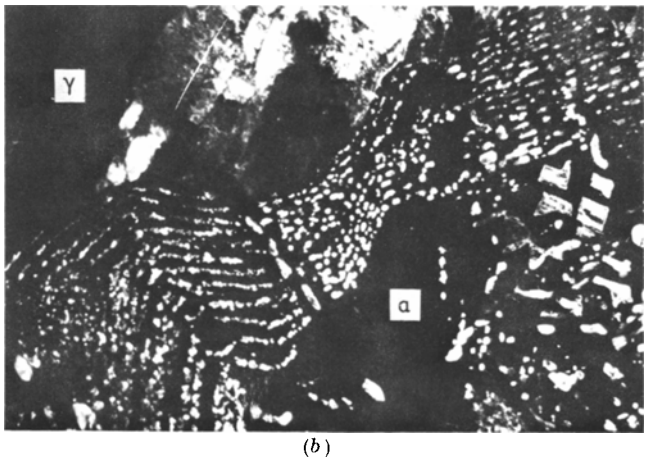

(*b*)

Fig. 8—An Fe-12 pct Cr-0.2 pct C alloy isothermally transformed for 60 min at 625°C. Thin foil electron micrograph, magnification 28,600 times. (*a*) bright field, (*b*) dark field (same area) using centered 220 $M_{23}C_6$ spot as direct beam. (Campbell).

transformed 5 min at 690°C in which the band spacing is within this range. The individual particles cannot be resolved in the electron microscope at this stage in this steel, but use of the field ion microscope allows their distribution and morphology to be studied,[27] Fig. 7.

2) The bands run parallel to the γ-α phase boundary and follow any sharp changes in direction of the ferrite growth front as shown in a partly transformed chromium steel, Fig. 8(*a*). The same field is shown in dark field using a centered {220} $M_{23}C_6$ spot as direct beam, Fig. 8(*b*).

3) The morphology of the carbide is usually the same as that adopted by the same alloy carbide in tempered martensite, except that frequently only one variant of the morphology is present, and that is often the one which allows the particles to be most closely parallel to the interface between γ and α.

These characteristics, together with a number of detailed structural observations, have led to the conclusion that the carbide particles are nucleated at the γ-α interface, and represent successive positions of the boundary as it sweeps through the structure. Variations of this basic mechanism have been suggested by several workers (Mannerkoski,[13] Relander,[14] Davenport *et al.*,[23] Gray and Yeo[19]) as the explanation of aligned carbide precipitates now frequently observed

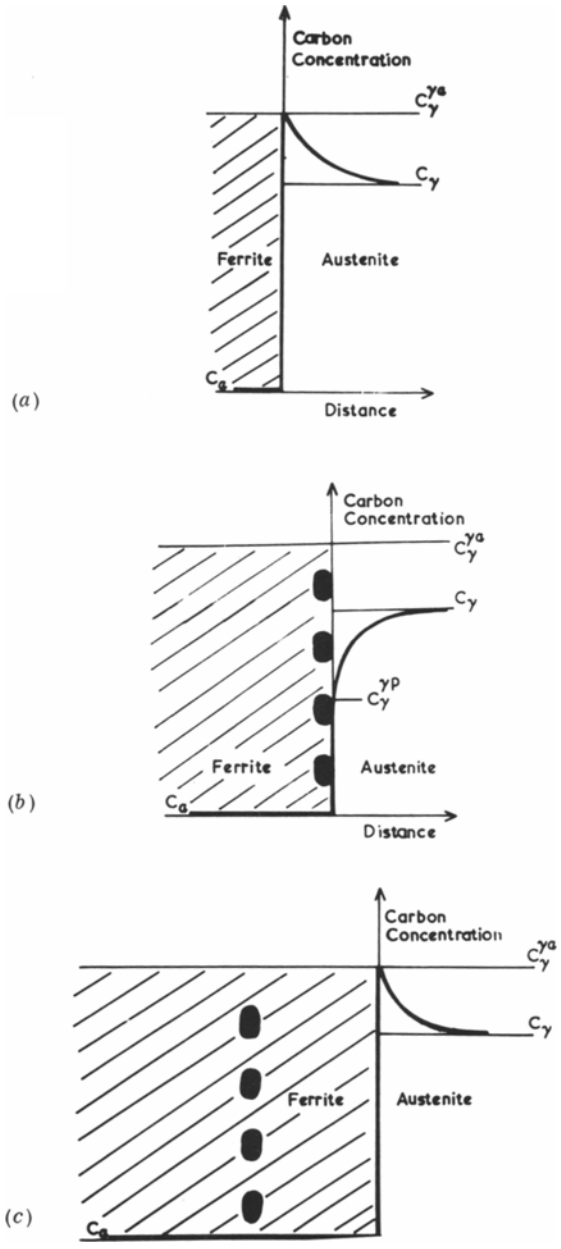

Fig. 9—Schematic model of interphase precipitation. In (*a*) partitioning of carbon occurs before precipitation coupled with a gradual build-up. In (*b*) the concentrations are sufficient for carbide nucleation on the ferrite side of the γ-α boundary which pins the boundary and depletes the adjacent austenite of carbon to some level C_γ^γ near the precipitate. Eventually the carbon depletion increases the driving force for ferrite formation sufficiently to drag the γ-α boundary away, (*c*), and the partitioning process recommences. (Davenport and Honeycombe).

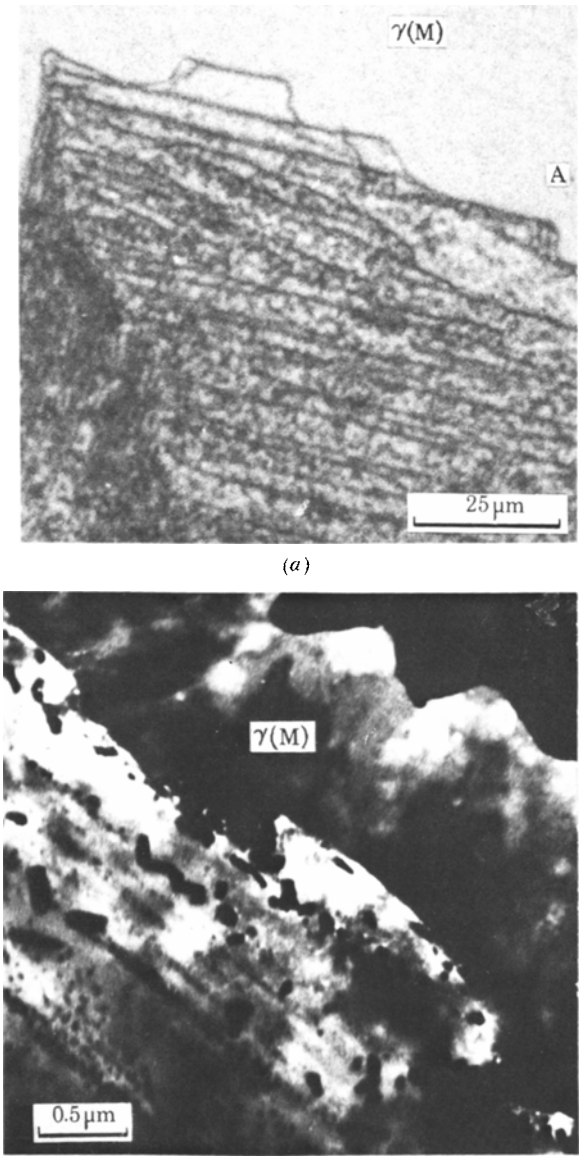

Fig. 10—An Fe-6 pct W-0.23 pct C alloy (*a*) transformed 2 hr at 800°C. Optical micrograph, magnification 750 times. (*b*) transformed 15 min at 750°C. Electron micrograph of transformation front showing M_6C precipitates. (Davenport and Honeycombe).

in ferrite. Davenport and Honeycombe[8] have suggested that the movement of the γ-α boundary is controlled by the carbon concentration ahead of the austenite, Fig. 9. When the ferrite boundary just reaches a new position for nucleation, there is a sharp partition of carbon across it, the austenite at the boundary is enriched to a critical value C_γ^α, while the adjacent ferrite has a carbon concentration C_α. In the extreme case the diffusion distances are only 2 nm (20Å), *e.g.* in an Fe-1V-0.2C steel transformed at 650°C, which is reflected in the extremely rapid rate at which the reaction occurs. At 700°C the transformation from $\gamma \rightarrow (\alpha$ + vanadium carbide) is complete in less than one minute, which does not allow for diffusion of metallic atoms over large distances, so the metallic solute atoms needed for carbide nucleation may well segregate by diffusion along the interface. It is also possible that solute atoms are collected in the γ-α boundary during movement, leading to a solute drag effect (Aaronson[24]), which would eventually halt the boundary, and allow nucleation to proceed.

In some steels, notably Fe-6 wt pct W-0.2 pct C and Fe-12 pct Cr-0.2 pct C, interphase precipitation and the associated growth of ferrite occurs on an extremely coarse scale, which allows a detailed study of the γ-α interface and the bands of precipitate. Such studies[8,9] have revealed two ways in which the interface moves:

1) The ferrite interface breaks away from the bands

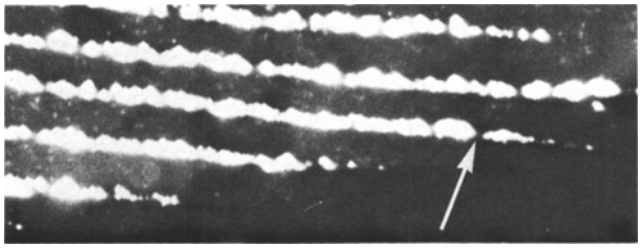

(*a*)

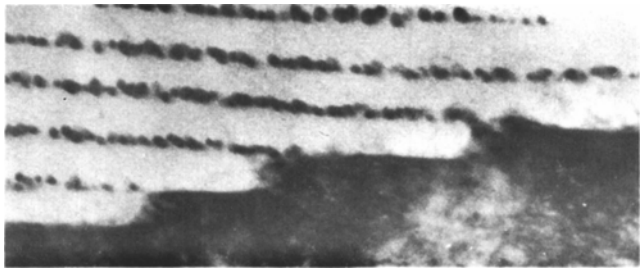

(*b*)

Fig. 11—An Fe-12 pct Cr-0.2 pct C alloy transformed 30 min at 650°C. (*a*) bright field electron micrograph, (*b*) dark field (same area) using a $M_{23}C_6$ reflection. The arrow indicates the position of one step and precipitation can be detected beyond it on the long section of the γ-α interface. Magnification 100,000 times. (Campbell).

of precipitate in localized loops which can sometimes be observed in the optical microscope, Fig. 10(*a*). The earlier positions of the interphase boundary in this Fe-W-C alloy are readily revealed by etching up the precipitate bands. Thin foil electron microscopy shows in greater detail this break away of the boundary from the last band of precipitate (M_6C) to form, Fig. 10(*b*), and in so doing provides new sites for further nucleation of M_6C. A break away of this type could "unzip" longer lengths of boundary by the movement of the two limiting steps in opposite directions.

2) Growth of the ferrite crystal can occur by movement of successive small steps along the γ-α boundary, usually all in the same direction. Mannerkoski,[13] and more recently Campbell,[9] have observed this phenomenon in high-chromium steels. An example is shown in an Fe-12 pct Cr-0.2 pct C alloy, Fig. 11(*a*), partially transformed after 10 minutes at 700°C, where bands of $M_{23}C_6$ are clearly associated with large steps in the ferrite. Dark field EM studies of such specimens show that the sites for carbide nucleation are not on the facets but on the long faces of the steps, Figs. 11(*a*) and (*b*). Precise crystallographic analysis of the steps is difficult, but Campbell has found that the planar interphase boundary could be $\{110\}_\alpha$ while the steps are consistent with $\{112\}_\alpha$. The $\{110\}_\alpha$ plane provides a low-energy coherent interface with $\{111\}_\gamma$ planes (Kurdjumov-Sachs), while the $\{112\}_\alpha$ step could be a high-energy interface capable of rapid movement, and thus unlikely to become a suitable site for carbide nucleation. Conversely, the $\{110\}_\alpha$ planar interface acts more effectively in nucleation because of its relative immobility.

3) Widmanstätten Ferrite[1]

While the long plates characteristic of Widmanstätten ferrite are often a striking feature of lower carbon steels, this type of structure is really only an extension of the side plate morphology of grain boundary ferrite idiomorphs, where the ferrite has an orientation with the austenite grain in which it grows, viz. the Kurdjumov-Sachs.

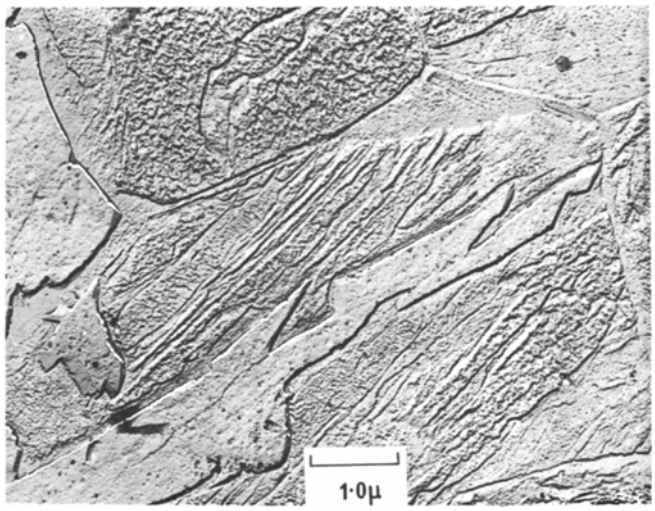

Fig. 12—First-formed upper bainitic ferrite lath in 0.1 pct C steel transformed at 600°C. Replica electron micrograph, magnification 12,000 times.

The plate morphology has been explained by several theories summarized in detail by Aaronson.[24] They vary from the diffusion geometry theory of Mehl and Barrett,[26] who assumed that the edges of plates grow more rapidly because of the steeper concentration gradients, to the lattice shear theories which are supported by the observation of surface relief effects (at least in bainitic ferrite).[27] In between these two extremes, there is a group of theories originating with Smith and Aaronson, in which the strongly anisotropic growth of Widmanstätten ferrite is explained in terms of the great ease of motion of incoherent phase boundaries compared with coherent ones. It seems likely in some circumstances that growth of the plates occurs by the movement of incoherent ledges on the coherent interfaces as postulated by Aaronson, and observed in some ferritic alloys. However, it is clear that no one theory can account for all the forms of Widmanstätten ferrite over the whole temperature range of formation, and that each of the above mechanisms may be operative under different circumstances.

4) Upper Bainite[28-30]

Nucleation occurs mainly at the austenite grain boundaries. The first formed transformation products are ferrite laths, Fig. 12, which nucleate rapidly by a sympathetic side-by-side reaction.[30] The ferrite grains therefore appear as sheaves of elongated grains, often with a small orientation difference between each unit. Surface relief effects similar to those produced by martensite are found, and although it is generally considered that a shear transformation is involved, the evidence is not unambiguous. Growth of the plates occurs predominantly along the major axis.

Upper bainitic ferrite contains a lower carbon content than the austenite from which it forms, although it is still supersaturated with respect to carbon. This supersaturation increases with decreasing transforma-

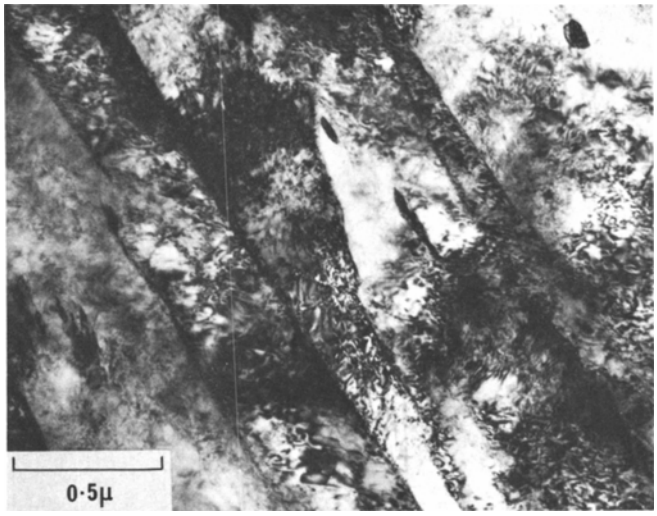

Fig. 13—Upper bainite in 0.1 pct C steel transformed at 550°C. Thin foil electron micrograph, magnification 38,000 times.

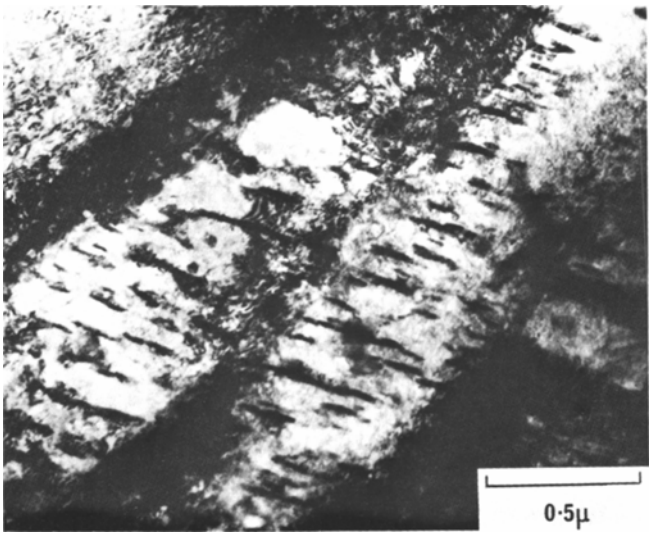

Fig. 14—Lower bainite in 0.6 pct C steel transformed at 300°C. Thin foil electron micrograph, magnification 48,600 times.

tion temperature, and consequently the austenite is enriched in carbon. In some cases, this carbon enrichment causes retention of untransformed austenite, particularly between two adjacent ferrite laths.[31] Due to this carbon enrichment, regions of high-carbon austenite transform eventually to carbide films which lie generally along the boundaries between adjoining ferrite grains, Fig. 13. With either increasing carbon content or decreasing transformation temperature, the width of the bainitic ferrite laths decreases, and consequently the carbides are closer together. With certain compositions and cooling rates, the carbon-enriched austenite does not transform to carbide films, but remains either as pools of retained austenite or high-carbon martensite between the bainitic ferrite grains.[32] This type of structure has been referred to as granular bainite. The upper bainitic ferrite contains an appreciable dislocation density which increases with decreasing transformation temperature.

In published studies on bainite, the carbide has been invariably Fe_3C. No work has apparently been done on the crystallography of upper bainite containing an alloy carbide. As shown by Shackleton and Kelly,[33] if the ferrite and cementite are both assumed to precipitate directly from the parent austenite with their respective orientation relationships, then the observed orientation relationships between the cementite and the bainitic ferrite can be rationalized. The orientation between upper bainitic ferrite and austenite appears to obey the Kurdjumov-Sachs relationship, the habit plane of the ferrite laths being $\{111\}_\gamma$. Usually, orientation differences between neighboring bainitic ferrite grains are observed, Fig. 13, this misorientation normally varying between 6 and 18 deg. There are many possible orientation variations for a ferrite grain formed from an austenite grain of given orientation. Six groups of such variants occur, the misorientation within any group being in the range referred to above, and between groups either 51, 97, or 120 deg.

5) Lower Bainite[28-30]

In lower bainite, nucleation again occurs at the prior austenite grain boundaries, but there is also a tendency for it to occur more frequently within the grains. Lower bainitic ferrite appears to form by shear, and there is evidence that the first formed lower bainitic lath is supersaturated with carbon[34] to a much greater extent than upper bainite. The growth of such bainitic ferrite proceeds with precipitation of carbide.[35] The laths grow mainly along their major axis, but there is also some lateral growth.

The carbide morphology is quite distinct from that of upper bainite insofar as it occurs within the individual ferrite laths. Moreover, within a given lath only one variant of a Widmanstätten morphology is observed,[36] Fig. 14. There is no sound evidence that twinning in the bainitic ferrite[33] is responsible for this carbide morphology. Indeed, it is more indicative of an interphase type of precipitation occurring during the growth of the laths. Lower bainitic ferrite invariably contains a considerable density of dislocations in complex and scarcely resolvable tangles.

The orientation relationship between the cementite and the lower bainitic ferrite has been reported as:[33]

$$(001)_{Fe_3C} \parallel (211)_\alpha$$

$$[100]_{Fe_3C} \parallel [0\bar{1}1]_\alpha$$

$$[010]_{Fe_3C} \parallel [1\bar{1}\bar{1}]_\alpha$$

This relationship is that obeyed by the precipitation of cementite from martensite during tempering, and also for cementite in quench aged ferrite. It appears that bainitic ferrite formation has similar crystallographic features to that of martensite, and the lower bainites in eutectoid steels have habit planes similar to those of higher-carbon martensites.

KINETICS

1) Ferrite

The kinetics of ferrite growth in plain carbon austenite have been shown to be determined by the diffussivity of carbon in austenite.[37] The addition of alloying elements in solid solution in the austenite is, however, crucial, as it has been shown theoretically that the composition of the austenite in contact with the fer-

rite is the most important factor in growth kinetics.[3,38] It has been concluded that partition of alloying elements between γ and α only occurs at higher temperatures, and below a certain critical temperature it does not occur at all. Kinsman and Aaronson[39] have found that this temperature is in some cases coincident with the Ae_3 temperature, and that no partition occurs in some systems, *e.g.* those containing Al, Co, Cu, Mo, and Si. Partition does occur below Ae_3 with Ni, Mn, and Pt. However, the findings on lack of partition are open to criticism as it may occur on a smaller scale than that indicated by microprobe analysis. Indeed the presence of very fine alloy carbide dispersions in some ferrites suggests that this is the case.

The effects of the various solute elements on nucleation and growth of ferrite have been rationalized in terms of their effect on the Ae_3 temperature relative to the Ae_3 temperature for a plain Fe-C alloy. An element which raises the Ae_3 temperature, increases the volume free energy change controlling the nucleation of α and also the concentration gradient, which provides the driving force for growth. Co, Al, and Si do in fact displace the ferrite reaction to shorter times in *TTT* diagrams; however, the behavior of molybdenum is anomalous. On the other hand, nickel and manganese lower the Ae_3 temperature and should therefore slow down the ferrite reaction, as they are observed to do.

Kinsman and Aaronson[39] have made a detailed comparison of the kinetics of an Fe-0.5 at. pct C alloy with those of an Fe-1.0 at. pct Mn-0.5 at. pct C and an Fe-1.0 at. pct Mo-0.5 at. pct C alloy. Typical *TTT* diagrams for the initiation of the reaction are shown in Fig. 15 which illustrates the expected behavior for manganese, but a marked difference in the case of molybdenum. These discrepancies can probably be accounted for by basic differences in the nature of the transformation product in the two alloys. Moreover, the two branches of the curve for the molybdenum steel may represent two separate reactions.

The same authors studied the thickening of ferrite allotriomorphs directly, by the use of thermionic emission microscopy, to determine whether the movement of the boundaries followed the relationship required by theory for a diffusion-controlled interface, viz.:

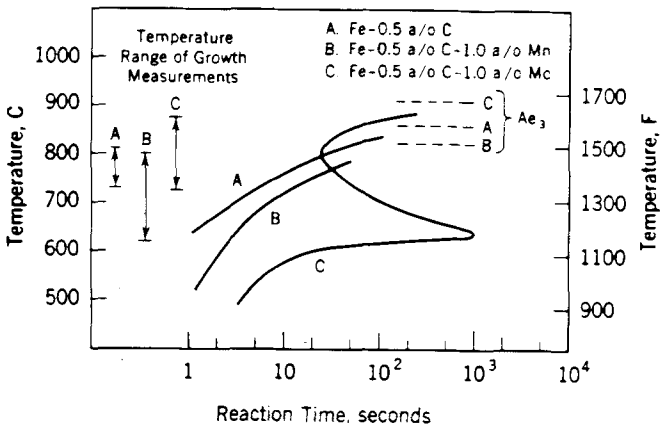

Fig. 15—Isothermal transformation diagrams for (*a*) Fe-0.5 at. pct C; (*b*) Fe-1 at. pct Mn-0.5 at. pct C; (*c*) Fe-1 at. pct Mo-0.5 at. pct C. (Kinsman and Aaronson).

$$T = \alpha t^{\frac{1}{2}}$$

where

T = thickness of allotriomorph

t = time

α = constant

They found that in all three alloys the thickness was linearly related to $t^{1/2}$. Determination of the constant α showed that it was in good agreement with the values calculated assuming that the rate controlling process is the volume diffusion of carbon in austenite.

2) Bainite

Many studies have been made of the kinetics of the bainite reaction, employing either resistivity or hot-stage microscope techniques. Both techniques can be criticized. Resistivity studies can be complicated by tempering occurring during the transformation. In hot-stage microstructural studies there is some doubt whether the surface relief quantitatively defines the boundaries of the transformed product, and also whether growth rates involve those of individual units or aggregates of bainitic plates. The thickening, and to some extent the lengthwise growth rates which are measured, may also be more controlled by the accommodation of the surface to the stresses set up than by the actual rates of growth.

Despite these uncertainties, there is general agreement that with more than ~0.5 pct C, a discontinuity in the reaction occurs at a temperature about 350°C. Above 350°C, upper bainite is formed, whilst below 350°C lower bainite is formed. It has also been reported[40] that the activation energies for upper and lower bainite formation are approximately those of carbon diffusion in austenite, and ferrite, respectively.

In lower-carbon steels however, the change from upper to lower bainite occurs at rather higher temper-

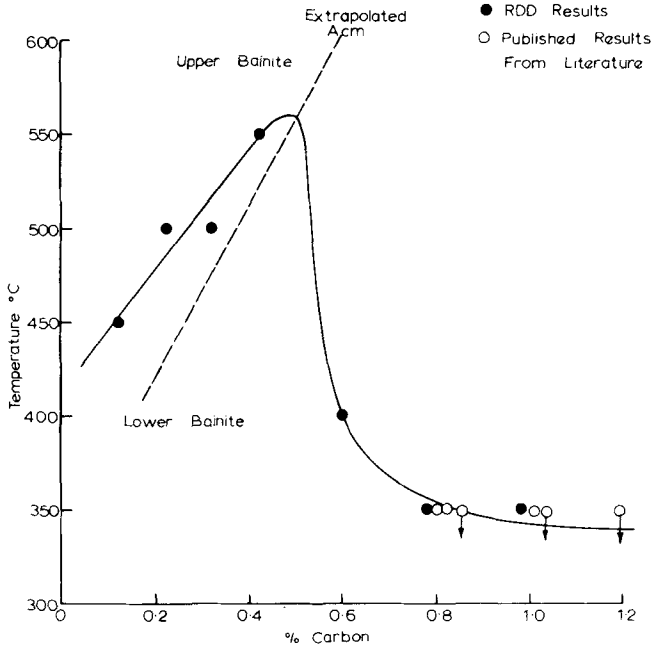

Fig. 16—The effect of carbon content on the change from upper to lower bainite.

atures than 350°C. The change from upper to lower bainite occurs over a range of temperatures, and at some temperatures there is a mixture of upper and lower bainite. The maximum temperature above which lower bainite is not observed is shown as a function of carbon content in Fig. 16.[30]

The extrapolation of the *Acm* line is also shown in Fig. 16. It is significant that when the steel becomes supersaturated with respect to cementite the temperature of the change from upper to lower bainite abruptly decreases and then remains constant for all higher-carbon compositions.

Recent kinetic studies[41,42] indicate that the diffusion controlled growth models, in which the growth of the bainite structural unit is controlled by the removal of carbon away from the bainite-austenite interface, are not operative. Rather it is suggested that both upper and lower bainite form by repeated nucleation of the individual structural units, and growth rates measured by hot-stage microscopy are controlled by this multiple nucleation process. This suggests that the growth of bainite is associated with the relief of transformation strains. Step quenching experiments have shown that lower bainitic ferrite plates do not continue to grow when the temperature is raised into the upper bainite range; rather new upper bainite laths are nucleated. Growth of both upper and lower bainite ceases when up-quenched to above B_s, but recommences on cooling to the original temperature.

Little or no work has been reported on the effect of alloying elements on the detailed kinetics of the bainite reaction, which is in contrast to the large volume of similar work on the ferrite reaction. However, information is available on the effect of alloying elements on the B_s temperature,[43] which is linearly depressed by alloying additions, and can be described by the following equation:

$$B_s\,^{\circ}\mathrm{C} = 830 - 270 \text{ pct C} - 90 \text{ pct Mn} - 37 \text{ pct Ni} - 70 \text{ pct Cr} - 83 \text{ pct Mo}$$

It has also been shown that the $B_{50\text{ pct}}$ and B_f temperatures occur at more or less fixed temperature intervals below B_s, *i.e.* the $B_s - B_f$ range for many steels is constant (about 120°C).

RATIONALIZATION OF SUBCRITICAL TRANSFORMATIONS IN AUSTENITE

There are two main factors which dominate all the transformations in alloy steels below Ae_1, namely:

i) the mechanism by which ferrite forms;
ii) the diffusivity of carbon and of the substitutional alloying elements.

At the highest temperatures, > 650°C, ferrite forms by a thermally-activated process of nucleation and growth at the austenite grain boundaries. The growth of the nuclei is achieved by atomic transfer across the γ-α interface, which occurs at an adequate rate at an incoherent interface. However, in the case of a coherent interface, where the Kurdjumov-Sachs relationship holds, growth occurs by the movement of steps along the interface. At intermediate temperatures, it is the authors' opinion that ferrite forms by a shear mechanism which in both Widmanstätten ferrite and upper bainite obeys the Kurdjumov-Sachs relationship with the austenite in which it is growing. In both these cases the residual austenite is enriched in carbon, but with Widmanstätten ferrite it transforms to pearlite, whilst in upper bainite a cementite film results because the transformation temperature is below that for pearlite formation. At the lowest temperatures, the transformation strains are such that the ferrite laths probably form by shear with irrational habit planes close to those of martensite.

Turning to the diffusional aspects of the transformations, it is clear that at the highest temperatures not only the carbon but also the other alloying elements are free to diffuse, so partitioning occurs. In the case of elements which form more stable carbides than iron, the carbon is normally precipitated as an alloy carbide, with several different morphologies. The pearlite and fibrous carbide morphologies arise from the nucleation of nodules at austenite grain boundaries, which subsequently grow into the austenite grain which is *not* crystallographically related to the ferrite. On the other hand, the interphase reaction occurs at both coherent and incoherent α/γ interfaces. Whilst the incoherent interfaces share the growth characteristics of the polyhedral ferrite and pearlite morphologies, the coherent interfaces need steps to achieve the necessary growth rates.

Whilst it is not yet possible to rationalize all the complex structural observations, it seems that the pearlitic alloy carbides and the fibrous alloy carbides are formed primarily under high-temperature conditions at incoherent high-energy interfaces, and represent a closer approach to equilibrium than the interphase morphologies. The tendency of some carbides to form coarse pearlitic structures rather than fibrous ones may be due to their more complex crystal structures. The interphase precipitation reaction, whilst it occurs over a wide temperature range in some steels, appears to provide the lowest temperature mechanism by which alloy carbides can form. At these lowest temperatures the ferrite is probably forming by shear and growing by step propagation along coherent interfaces with alloy carbide nucleation occurring at the steps. As far as carbide formation is concerned, the bainites provide a useful analogy with the higher temperature transformation products in alloy steels. In both upper and lower bainite, cementite is the predominant carbide because the transformation temperatures are too low for the substitutional alloying elements to diffuse—*cf.* the tempering behavior of alloy martensites. Furthermore, the cementite morphology adopted is determined by the diffusivity of the carbon. In upper bainite the diffusion of carbon in untransformed austenite is sufficiently rapid to allow complete partition between the ferrite and the austenite; the residual austenite finally deposits cementite as continuous or semicontinuous films between bainitic ferrite laths, giving a structure not unlike fine pearlite, Fig. 17. The carbon diffusion during the formation of lower bainite is so restricted that carbon concentrations build up at the γ/α interface leading to the nucleation of small cementite particles. Here is a clear analogy to the interphase precipitation of alloy carbides at higher temperatures. The unique habit of the cementite particles (*cf.* V_4C_3 *in ferrite*) is strong sup-

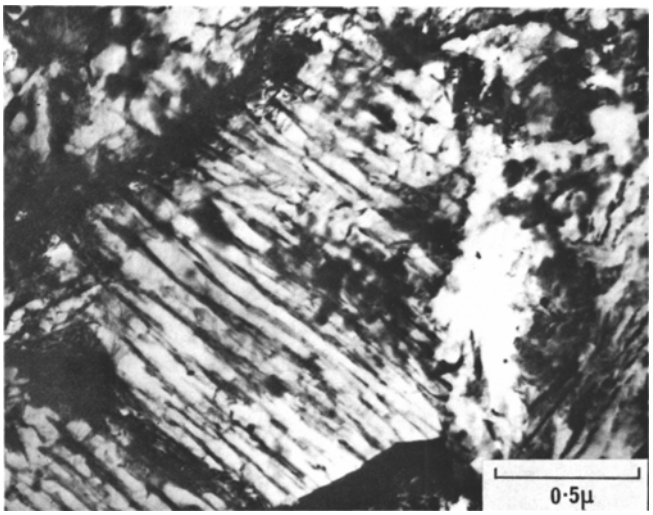

Fig. 17—Higher-carbon upper bainite in 0.6 pct C steel transformed at 500°C, showing resemblance to fine pearlite. Thin foil electron micrograph, magnification 37,500 times.

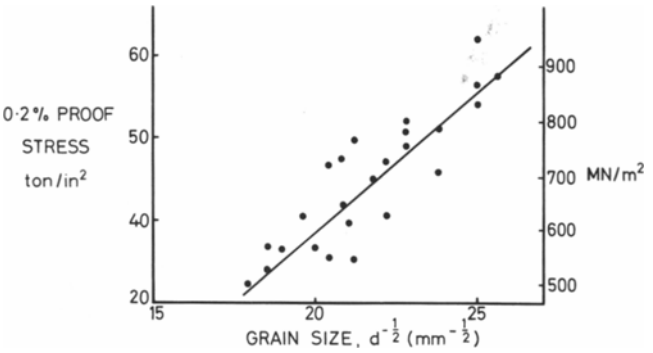

Fig. 18—The effect of bainitic ferrite grain size on the proof stress (Pickering).

port for their nucleation at an interface, and their actual orientation is compatible with their growth in ferrite, insofar as the orientation relationship is the same as that for cementite precipitated in tempered martensite.

MECHANICAL PROPERTIES

1) Strengthening Effects and Mechanisms

Much work has been done to identify the strengthening mechanisms in both ferrite and bainite. In ferrite, the work has been largely confined to plain carbon or grain refined steels. In bainitic structures, the work on strengthening mechanisms has been largely done on low-alloy steels as such steels enable the appropriate microstructures to be more readily obtained Various strengthening mechanisms can be identified:

1.1) The Ferrite Grain Size

It is well known that refining the ferrite grain size in polygonal ferrite structures increases the yield strength according to the Hall-Petch equation[44]

$$\text{Yield Stress} = \sigma_0 + k\, d^{-\frac{1}{2}}$$

where d = ferrite grain diameter.

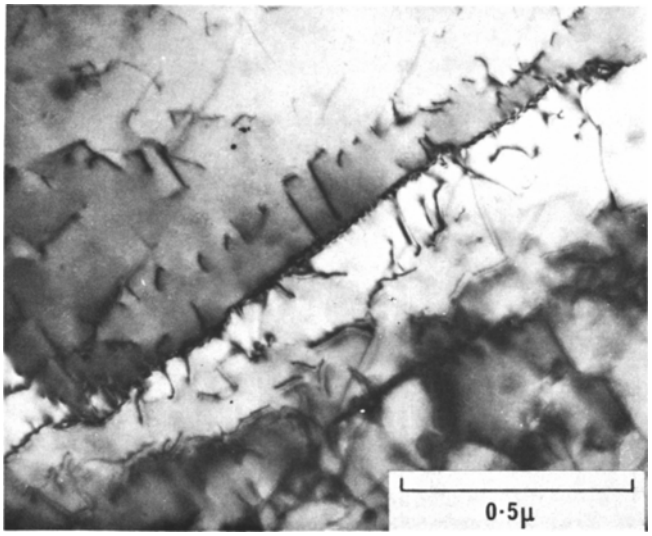

Fig. 19—Bainitic ferrite boundary in 0.1 pct C steel transformed at 650°C. Thin foil electron micrograph, magnification 61,000 times.

For bainitic ferrite it can also be seen that there is a similar relationship, Fig. 18.[50] It is clear that the bainitic ferrite grain size is a major factor controlling the strength, and it is interesting that the bainitic ferrite boundaries, Fig. 19, are apparently able to impede dislocation movement sufficiently to increase the yield stress.

1.2) Dispersion Strengthening by Carbides

The interphase reaction has been shown to have a substantial strengthening effect on ferrite. For a given particle size distribution, the intensity of strengthening is related to the volume fraction of dispersed carbide. Recent developments in mild steels containing small additions of niobium, vanadium, and so forth, use both grain refinement and dispersion strengthening by alloy carbides to achieve high strength levels. The dispersion strengthening, which in this case leads to strength increments of up to 150 MN m^{-2} (10 t.s.i.) have now been shown to result from interphase precipitation of NbC, V_4C_3, and so forth during transformation to ferrite. Recent work[45] on both commercial steels and experimental alloys,[17] has shown that the strengthening so achieved can be interpreted in terms of a modified Orowan-Ashby model. In bainitic structures the strength increases as the cementite dispersion is refined, Fig. 20. However, in upper bainitic structures the carbides are mainly on the bainitic ferrite grain boundaries where they do *not* greatly contribute to the strength but adversely affect the toughness 1.3)

1.3) Dislocation Density

The polygonal ferrite formed at high temperatures contains a very low dislocation density, although there is an increase in the number of dislocations as the transformation temperature is lowered. The effect on strength is, however, small, and at best does not contribute more than 30 MN m^{-2} (~2 t.s.i.) to the yield strength.[46] It has been shown that the flow stress of ferrite is related to the square root of the dislocation

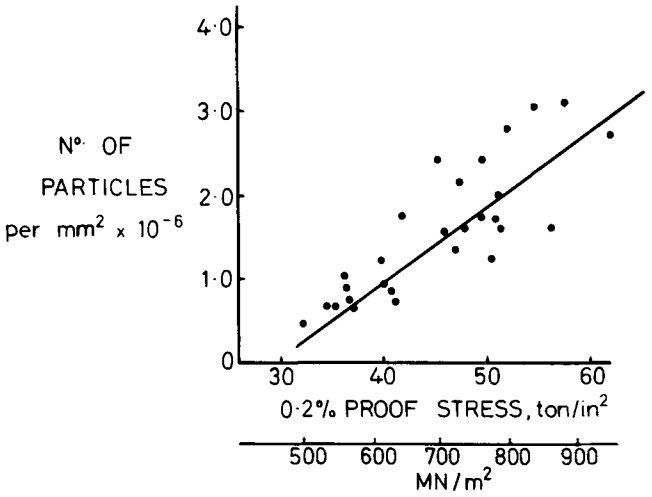

Fig. 20—The effect of carbide particles on the proof stress of bainitic steels.

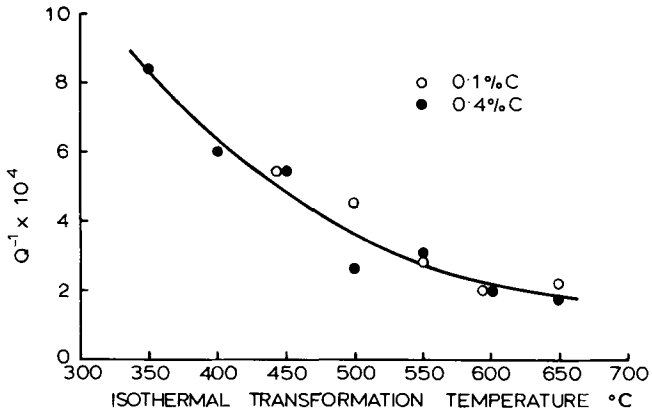

Fig. 21—The effect of transformation temperature on the internal friction (Koster) peak in bainite.

density. As the mechanism of ferrite formation changes to shear, the dislocation density increases substantially and so dislocations make a significant contribution to the strength. As will be shown later, there is evidence to indicate that many of the dislocations are associated with "atmospheres" of carbon atoms.

1.4) Carbon Dissolved in Ferrite

In polygonal ferrite, particularly in commercially heat-treated materials in which the rate of cooling is relatively slow, there is little carbon retained in solid solution. This is particularly the case when alloy carbides are precipitated, as the solubility of carbon is then further decreased. Consequently carbon dissolved in ferrite has little strengthening effect unless a definite attempt has been made to retain it in solution by quenching immediately after the transformation.

Published evidence[34] indicates that with decreasing transformation temperature the bainitic ferrite becomes supersaturated with carbon. This tends to produce solid solution strengthening, which may partly be due to an association of the dissolved interstitial carbon atoms with the dislocations. Such an association of carbon atoms with dislocations is shown by internal friction experiments,[30] Fig. 21, in which the intensity

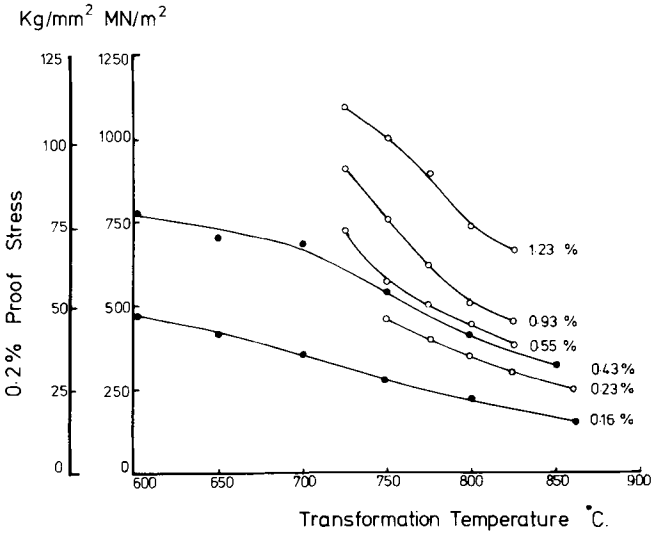

Fig. 22—The effect of volume fraction carbide and transformation temperature on the yield strengths of isothermally-transformed steels. Titanium steels ●; vanadium steels ○.

of the Koster peak is a function of the interaction between dislocations and interstitial atoms.

1.5) Solid Solution Strengthening

Solid solution effects have been clearly shown to play some part in increasing the yield strength of ferrite. In general the effects are not large, especially for substitutional solutes, and in many cases the amount of solute which can be added is limited due to the fact that ferrite formation is suppressed by the increasing hardenability. Undoubtedly, substitutionally dissolved solutes will also tend to increase the strength of bainite, but would be expected to play an even less significant role in the higher-strength bainite than in polygonal ferrite.

2) Structure-Property Relationships in Ferrite

2.1) Simple Iron Alloys

The effects of strengthening ferrite by interphase carbide precipitation have been studied in vanadium steels[17,47] and in titanium steels.[21] Other things being equal, for the same volume fractions of precipitate (V_4C_3 or TiC) the strengthening effect on the ferrite is roughly the same, higher strengths being obtained in vanadium steels because austenite dissolves a higher volume fraction of V_4C_3 than of TiC. The effect of isothermal transformation temperature for a series of vanadium steels, and a titanium steel, on the proof stress is shown in Fig. 22. These results illustrate clearly not only the effect on the mechanical properties of volume fraction of carbide, but also that of dispersion size as determined by the particular transformation temperature.

The dispersions produced by interphase precipitation are nonrandom, so it is not surprising that the unmodified Orowan theory of yielding cannot be applied. It is perhaps less obvious that an impenetrable wall model (analogous with a pearlite-type structure) is also not entirely satisfactory. This gives a relationship of the type $\Delta\tau = \kappa\lambda^{-0.5}$, where $\Delta\tau$ = increase in

yield stress; λ = spacing between walls, whereas interphase precipitation alloys give values of the exponent closer to 0.7. One thus comes to the conclusion that the strengthening process is intermediate between that of a simple precipitation hardening reaction and a pearlitic process

Batte[17] has further shown that the work-hardening behavior of interphase precipitation-strengthened ferrite is complex. The initial dislocation population of the ferrite is low (in contrast to bainite and tempered martensite), and up to about 2.5 pct strain the low work-hardening rate increases with the coarseness of the dispersion, qualitatively following the Fisher, Hart, and Frye theory.[48] However, at higher strains (above 2.5 pct) the theory of Ashby,[49] which is based on the initiation of cross-slip at particles, more closely accounts for the observed work-hardening rates:

$$\frac{d\tau}{d\gamma} = 0.12\,G\left(\frac{bf}{\gamma a}\right)^{1/2}$$

where

f = vol. fraction of precipitate

a = particle diameter

G = shear modulus of matrix

γ = shear strain

τ = stress

It predicts, as observed, a higher work-hardening rate for smaller particles, at a given shear strain and volume fraction.

2.2) Commercial Steels

Useful empirical equations have been derived for the yield stress, tensile strength, and impact transition temperatures of low-alloy ferritic steels strengthened by solutes and grain size:

$$\text{Yield Stress, t.s.i.} = 3.5 + 2.1(\text{pct Mn}) + 5.4(\text{pct Si}) + 23(N_f) + 1.13(d^{-1/2})$$

$$\text{Tensile Strength, t.s.i.} = 19.1 + 1.8(\text{pct Mn}) + 5.4(\text{pct Si}) + 0.5(d^{-1/2}) + 0.25(\text{pct pearlite})$$

$$\text{Impact Transition Temperature, °C} = -19 + 44(\text{pct Si}) + 700(N_f) - 11.5(d^{-1/2}) + 2.2(\text{pct pearlite})$$

where

N_f = Nitrogen not combined as a stable nitride.

Using these equations it is also possible to assess the solid solution effects of both substitutional and interstitial solutes, which are summarized in Table I.

Recent work[45] has allowed the dispersion strengthening to be compared with the predictions of the Orowan-Ashby model, suitably modified. In general the dispersion strengthening of 3 nm diam NbC particles is in close accord with the predictions. In the case of V_4C_3 precipitates there is a range of particle sizes from 3 nm to 300 nm, depending upon the degree of overaging. The largest particles give no strengthening, whilst the smallest particles can contribute about 150 MN m^{-2} (10 t.s.i.) to the yield stress. Thus it is now possible to describe satisfactorily the dispersion strengthening effects for a variety of carbide precipitates in ferrite, on a semiquantitative basis.

Table I. Effect of Solutes on Strength and Impact Properties

Element	Change in Property per Wt Pct of Element: Yield Stress, t.s.i.	Tensile Strength, t.s.i.	Impact Transition Temperature, °C
Carbon	300	430	–
Nitrogen	300	430	Not linear
Phosphorus	44	44	400
Tin	9	–	150
Silicon	5.4	5.4	44
Copper	2.5	0.6	N.D.
Manganese	2.1	1.8	0
Molybdenum	0.7	3.0	N.D.
Nickel	0	0.6	N.D.
Chromium	−2.0	−1.9	N.D.
Aluminum	–	–	75

3) Structure–Property Relationships in Bainite

Quantitative relationships between the microstructure and the strength are difficult to define because of the many interacting factors. An attempt has however been made[50] to obtain a relationship between the proof stress and microstructural parameters, *i.e.* bainitic ferrite grain size (d) and number of carbide particles per unit planar area of the structure (n). Much previous work has shown that the proof stress is related to the function, $d^{-1/2}$, and to a similar function of the planar interparticle spacing (S). The relationship between S and n is given by:

$$S = \frac{2}{(\pi n)^{1/2}} = 1.13\,n^{-1/2}$$

$$S^{-1/2} = \frac{(\pi n)^{1/4}}{2} = 0.941\,n^{1/4}$$

A multiple linear regression analysis gave the following equation for the 0.2 pct Proof Stress:

$$\text{0.2 pct Proof Stress (t.s.i.)} = -12.6 + 1.13\,d^{-1/2} + 0.98\,n^{1/4}$$

where both d and n are measured in mm.

The empirical nature of this analysis is shown by the negative constant which indicates a threshold carbide distribution beyond which carbides do not contribute to the strength. This is compatible with the suggestion that carbides do not contribute much to the strength of upper bainite because they occur largely at bainitic ferrite grain boundaries. Using this relationship the contributions of the grain size and carbide dispersion to the proof stress are shown in Fig. 23.

APPLICATIONS AND DEVELOPMENTS

a) Ferritic Steels

The fine carbide dispersions produced in ferrite by interphase precipitation during transformation have considerable potential as a means of strengthening low-alloy steels in a simple manner. While the high-strength mild steels to which niobium and/or vanadium

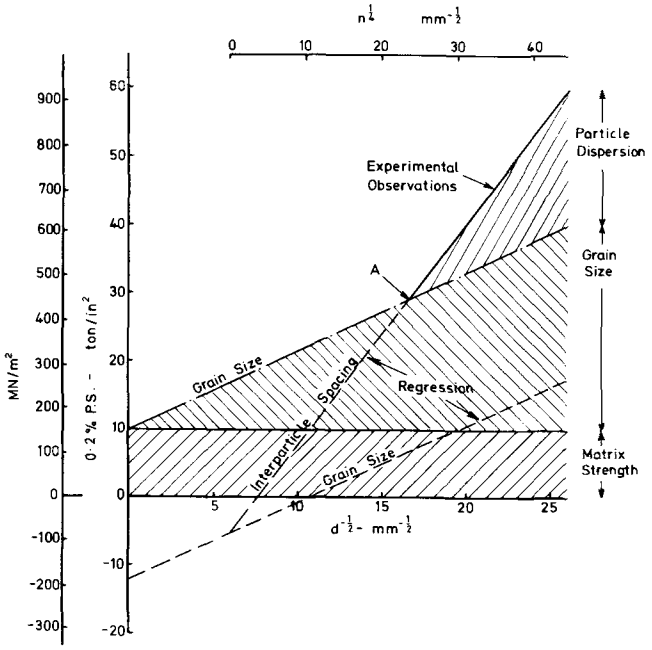

Fig. 23—The components of the strength of bainite.

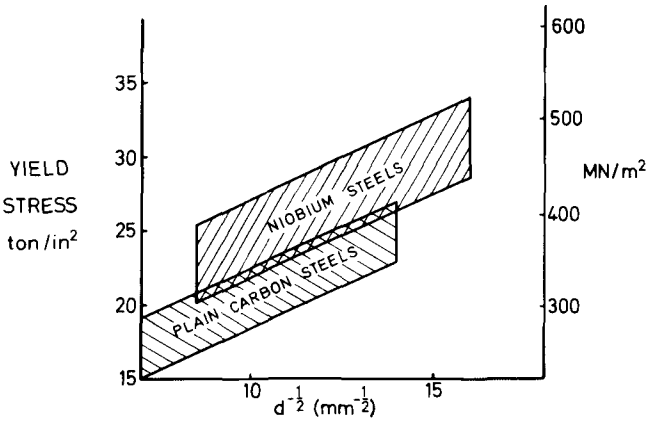

Fig. 24—The effect of grain size on the yield strength in controlled rolled plain carbon and niobium precipitation hardened steels (Irvine).

have been added in concentrations up to 0.1 wt pct owe much of their strength to the fine ferritic grain size achieved by carbide particles which limit grain growth, and by controlled rolling subsequently, there is a substantial additional strengthening due to the dispersion of alloy carbides produced during cooling through the transformation. Irvine[51] has shown for a 0.1C-0.5Mn steel that the presence of 0.02 wt pct Nb raises the yield stress at constant grain size by about 100 MN m^{-2} (~7 t.s.i.). Fig. 24 illustrates this effect for mild steels of different grain sizes with and without 0.02 wt pct Nb. Metallographic evidence for extensive interphase precipitation of NbC and V_4C_3 in this type of steel is now available.[19]

Straatman *et al.*[52] have reported a doubling of the yield strength of low-carbon hot-rolled steels as a result of the addition of 0.04 to 0.3 wt pct Ti. Recent work by Freeman[21] indicates that interphase precipitation of TiC occurs readily in similar alloys, and that it makes a substantial contribution to the strength achieved.

It thus seems clear that a new group of low alloy steels could be developed in which for a given grain size substantial additional strengthening is achieved by carbide precipitation during the phase transformation. In laboratory experiments, isothermal transformations have been used to study the basic physical metallurgy; however, in practice, cooling at standard rates following controlled rolling would achieve high strength levels. One of the present authors has advocated[47] the use of steels based on vanadium to make best use of the phenomenon, although the additional use of titanium may well be effective. Yield strengths in the range 300 to 750 MN m^{-2} (20 to 50 t.s.i.) can be easily achieved, and with proper control of grain size by controlled rolling, adequate toughness should also be obtained. In the long run this could be an easier heat treatment route than the traditional process of quenching followed by tempering, with its familiar hazards.

b) Bainitic Steels

For a useful bainitic steel we require

i) a low carbon content to obtain good weldability, toughness, and formability;

ii) proof stress values from 460 MN m^{-2} (30 t.s.i.) to 920 MN m^{-2} (60 t.s.i.);

iii) to obtain these properties by air cooling either directly from the finishing rolling temperature or by a simple normalizing treatment;

iv) to obtain the required properties, with a minimum of variation, over a wide range of section sizes.

These features require a metastable austenite bay between the ferrite and bainite C-curves, a rapid bainite reaction and a much retarded ferrite reaction. The bainite reaction should exhibit a flat-topped "C" curve. These requirements were most economically achieved in a low-carbon, $\frac{1}{2}$ pct Mo steel containing boron,[53] although other alloying combinations may be used, and very low carbon contents improve the impact properties.[54,55] The introduction of alloying elements into the $\frac{1}{2}$ pct Mo-B steels depresses the B_s-B_f range, and strengths from 460 to 920 MN m^{-2} (30 to 60 t.s.i.) proof stress can be produced.[56]

There is a limit to the amount of alloy which can be introduced because:

i) the depression of the transformation on cooling tends to form martensite so that the weldability of the steel is impaired;

ii) the bainitic reaction itself is so retarded that the steel becomes martensitic, air-hardening in the smaller section sizes. This effect is of great importance in the development of higher-carbon bainitic steels.[57]

Nevertheless, steels have been developed for a wide range of applications.[30,58] In addition, higher-carbon bainitic steels have been developed[57] containing up to 0.55 pct C. The range of analyses, and the ability to use other alloying elements to increase the strength, is restricted because combinations of alloying elements and carbon retard the bainite transformation, so that bainite can only form in limited section sizes.

Possible developments in bainitic steels include the use of low finishing temperatures, which might improve both the strength and ductility, particularly with respect to fracture toughness in thin sections. Finishing temperatures as low as 500°C produce only a slight

increase in strength, but the impact properties of the higher strength upper bainites can show a marked improvement due to a further refinement of the prior austenite grain size. Furthermore, beneficial effects are produced if the deformation is carried out in a narrow temperature range just above the B_s temperature. This is in effect an ausforming treatment, but other results on ausforming bainitic steels have shown that the increase in strength is relatively small and is very dependent on the transformation temperature of the steel, because of recovery in the austenite and annealing in the bainite either during or after transformation. Large ausforming reductions are required for an appreciable strength increase.

It may also be beneficial to use a precipitation reaction, if possible in air-cooling structures. Niobium would be expected to give slightly higher strength in the as-rolled condition, any benefit being lost in the normalized condition because of the limited solubility of niobium carbide in the austenite. The maximum strengthening effect would however be quite small, *i.e.* 75 MN m^{-2} (5 t.s.i.) on the proof stress. An alternative age-hardening addition is copper. This could give approximately 150 MN m^{-2} (10 t.s.i.) increase in the proof stress, but in steels containing about $1\frac{1}{2}$ pct Cu, a separate aging treatment would be necessary. If, however, 3 pct Cu could be accommodated in a bainitic steel without impairing the transformation characteristics, this would result in age hardening during normalizing, or in the as-rolled condition. Such an effect could only be produced if the transformation temperature was above the temperature at which copper precipitates. Recent work has confirmed that a copper-bearing bainitic steel is feasible, and indeed such a steel, but with low copper content, was developed many years ago.[59]

Finally, it seems that a bainitic steel could be used in the quenched and tempered condition in plate. This would enable any lack of hardenability to be counteracted by the fact that even in the air-cooled condition, bainite would be formed. Thus inefficient quenching would not be so deleterious and the properties across the section might be more uniform. Information on this type of development has recently been published.[60,61]

ACKNOWLEDGMENTS

One of the authors (F. B. P.) wishes to thank Dr. K. J. Irvine, Head of Research, Special Steels Division, British Steel Corporation, for permission to publish some of the results included in this paper. The other author thanks his colleagues, Dr. A. D. Batte, Dr. K. Campbell and Mr. S. Freeman for the use of unpublished information and photographs. He would also like to gratefully acknowledge the support of the Science Research Council (U.K.) and of the British Steel Corporation given to his research group in Cambridge.

REFERENCES

1. R. F. Mehl and A. Dubé: *Phase Transformation in Solids*, John Wiley & Sons, 1951.
2. H. I. Aaronson: in *Decomposition of Austenite by Diffusional Processes*, p. 387, Interscience, New York, 1962.
3. H. I. Aaronson, K. A. Domian, and G. M. Pound: *Trans. TMS-AIME*, 1966, vol. 236, p. 768.
4. C. S. Smith: *Trans. ASM*, 1953, vol. 45, p. 533.
5. G. Kurdjumov and G. Sachs: *Z. Physik*, 1930, vol. 64, p. 325.
6. M. Hillert: in *Decomposition of Austenite by Diffusional Processes*, p. 197, Interscience, New York, 1962.
7. H. I. Aaronson, C. Laird, and K. R. Kinsman: in *Phase Transformations*, p. 313, ASM, 1970.
8. A. T. Davenport and R. W. K. Honeycombe: *Proc. Roy. Soc.*, 1971, vol. A322, p. 191.
9. K. Campbell: Ph.D. Dissertation, University of Cambridge, 1971.
10. J. W. Cahn and W. C. Hagel: in *Decomposition of Austenite by Diffusional Processes*, p. 131, Interscience, New York, 1962.
11. R. I. Entin: in *Decomposition of Austenite by Diffusional Processes*, p. 295, Interscience, New York, 1962.
12. R. F. Mehl and W. C. Hagel: *Progr. Metal Phys.*, 1956, vol. 6, p. 74.
13. M. Mannerkoski: *Acta Polytech. Scand.*, 1964, Ch. 26.
14. K. Relander: *Acta Polytech. Scand.*, 1964, Ch. 34.
15. J. McCann and K. A. Ridal: *J. Iron Steel Inst.*, 1964, vol. 202, p. 441.
16. F. G. Berry and R. W. K. Honeycombe: *Met. Trans.*, 1970, vol. 1, p. 3279.
17. A. D. Batte: Ph.D. Dissertation, University of Cambridge, 1970.
18. W. B. Morrison: *J. Iron Steel Inst.*, 1963, vol. 201, p. 317.
19. J. M. Gray and R. B. G. Yeo: *Trans. ASM*, 1968, vol. 61, p. 255.
20. S. Freeman: Ph.D. Dissertation, University of Cambridge, 1971.
21. S. Freeman: *BSC/ISI Conf. on "The Effect of Second-Phase Particles on the Mechanical Properties of Steels"*, Paper 19, Scarborough, March 1971, p. 152.
22. D. M. Schwartz and B. Ralph: *Phil. Mag.*, 1969, vol. 19, p. 1061.
23. A. T. Davenport, F. G. Berry, and R. W. K. Honeycombe: *Met. Sci. J.*, 1968, vol. 2, p. 104.
24. H. I. Aaronson: *Inst. Metals Monograph, The Mechanism of Phase Transformations in Crystalline Solids*, 1969, no. 33, p. 220.
25. R. F. Mehl, C. S. Barrett, and D. W. Smith: *Trans. AIME*, 1953, vol. 105, p. 215.
26. R. F. Mehl and C. S. Barrett: Discussion to Ref. 4.
27. T. Kô and S. A. Cottrell: *J. Iron Steel Inst.*, 1952, vol. 172, p. 307.
28. E. S. Davenport and E. C. Bain: *Trans. AIME*, 1930, vol. 90, p. 117.
29. R. F. Hehemann: in *Phase Transformations*, p. 397, ASM, 1970.
30. F. B. Pickering: in *Transformation and Hardenability in Steel*, p. 109, Climax Molybdenum Co. of Michigan, Inc., 1967.
31. J. M. Wheatley and R. G. Baker: *Brit. Weld. J.*, 1963, vol. 10, no. 1, p. 23.
32. L. J. Habraken and M. Economopoulos: in *Transformation and Hardenability in Steels*, p. 69, Climax Molybdenum Co. of Michigan, Inc., 1967.
33. D. N. Shackleton and P. M. Kelly: *Iron Steel Inst. Spec. Rep. No.* 93, p. 146, 1965.
34. P. Vasudevan *et al.*: *J. Iron Steel Inst.*, 1958, vol. 190, p. 386.
35. G. R. Srinivasan and C. M. Wayman: *Acta Met.*, 1968, vol. 16, pp. 609, 621.
36. Y. Ohmori: *Trans. Iron Steel Inst. Japan*, 1971, vol. 11, p. 95.
37. C. Zener: *J. Appl. Phys.*, 1949, vol. 20, p. 950.
38. J. S. Kirkaldy: *Can. J. Phys.*, 1958, vol. 36, p. 907.
39. K. R. Kinsman and H. I. Aaronson: in *Transformation and Hardenability in Steels*, p. 109, Climax Molybdenum Co. of Michigan, Inc., 1967.
40. S. V. Radcliffe and E. C. Rollason: *J. Iron Steel Inst.*, 1959, vol. 191, p. 56.
41. R. H. Goodenow *et al.*: *Iron Steel Inst. Spec. Rep.*, 1965, no. 93, p. 135.
42. J. M. Oblak and R. F. Hehemann: in *Transformation and Hardenability in Steels*, p. 15, Climax Molybdenum Co. of Michigan, Inc., 1967.
43. W. Steven and A. G. Haynes: *J. Iron Steel Inst.*, 1956, vol. 183, p. 349.
44. N. J. Petch: *J. Iron Steel Inst.*, 1953, vol. 173, p. 25.
45. T. Gladman, B. Holmes, and I. D. McIvor: *BSC/ISI Conf. on "The Effect of Second-Phase Particles on the Mechanical Properties of Steels"*, Paper 9, Scarborough, March 1971, p. 68.
46. T. Gladman: British Steel Corporation, Swindon Laboratories, Rotherham, U.K., private communication, 1971.
47. R. W. K. Honeycombe: *BSC/ISI Conf. on "The Effect of Second-Phase Particles on the Mechanical Properties of Steels"*, Scarborough, March 1971, p. 136.
48. J. C. Fisher, E. W. Hart, and R. R. Pry: *Acta Met.*, 1953, vol. 1, p. 336.
49. M. F. Ashby: Proc. Second Bolton Landing Conference, 1968, p. 143.
50. T. Gladman: British Steel Corporation, Swindon Laboratories, Rotherham, U.K., private communication, 1971.
51. K. J. Irvine: *Iron and Steel*, February 1971, p. 31.
52. J. A. Straatman, R. A. Bosch, and W. R. Herrastein: Youngstown Sheet and Tube Company, Ohio. Paper presented at the 97th AIME meeting in 1968, unpublished work.
53. K. J. Irvine *et al.*: *J. Iron Steel Inst.*, 1957, vol. 186, p. 54.
54. A. J. McEvily *et al.*: in *Symp. on "Transformations and Hardenability in Steel"*, p. 179, Climax Molybdenum Co., 1967.
55. A. J. McEvily and C. L. Magee: *Iron Steel Inst. Publ. No.* 114, p. 111, 1968.
56. K. J. Irvine and F. B. Pickering: *J. Iron Steel Inst.*, 1957, vol. 187, p. 292.
57. K. J. Irvine and F. B. Pickering: *Iron Steel Inst. Spec. Rep. No.* 93, 1965, p. 110.
58. F. B. Pickering: in *Metallurgical Achievements*, p. 109, Pergamon Press, 1965.
59. R. F. Mehl and A. Rose: *Stahl und Eisen*, 1954, vol. 74, p. 1054.
60. R. L. Cryderman *et al.*: *Trans. ASM*, 1969, vol. 62, p. 561.
61. A. P. Coldren *et al.*: in *Steel Strengthening Mechanisms*, Climax Molybdenum Symp., Zurich, 1969, p. 17.